IOSR Journal of Mechanical and Civil Engineering (IOSR-JMCE)
e-ISSN: 2278-1684,p-ISSN: 2320-334X, Volume 13, Issue 3 Ver. VI (May- Jun. 2016), PP 34-49
www.iosrjournals.org

Structrual Analysis of Concrete Beams Reinforced with Basalt FRP Bars

Mohamed A. A. El-Shaer
Associate Professor, Civil and Construction Engineering Department, Higher Technological Institute, 10th of Ramadan City, EGYPT

Abstract: *The design codes for fiber-reinforced polymer (FRP) reinforced concrete beams do not consider the stringthing with Basalt fiber-reinforced polymer (BFRP) bars, where new material. As it is a new material, in this paper, a non-linear finite element analysis (FEA) has been done to analyze the flexural analysis of reinforced simple concrete beam strengthened with (BFRP) bars under short-term static vertical loads. Finite Element Model ANSYS 12.0 has been used to analyze the three-dimensional model. The reliability of the model was demonstrated by comparison with experimental results of concrete beam strengthened with BFRP bars carried out by another author, and the theoretical prediction agrees well with the test results. The study of the proposed analysis for two group of beams, the first with one load in mid-span, the second with tow loads at third-span and included many effects such as ultimate load, load-deflection response, ductility versus reinforcement ratio of BFRP bars, ultimate concrete stress and Ultimate tensile force in bars. The strategy for replacement the traditionally steel reinforced bars by BFRP bars has remarkably increased the ultimate load and ductility of the concrete beams by about 34% to 53%, decrease the max. deflection by about 30%, increase the ultimate tensile force in bars by about 82% to 104%, increase the ultimate concrete stress by about 220% to 268%.*

Keywords: *Basalt fiber-reinforced polymer (BFRP) bars; Deflections; Flexure behavior; Cracks; Reinforcement Concrete Beam (RCB); Finite Elements Analysis (FEA).*

I. Introduction

Durability of building structures is one of the most important features of present design [1]. Standard steel bars do not have corrosion resistance, hence traditional RC structures are very sensitive to damage in aggressive environment [2]. This problem does not affect in the FRP bars [3,4].FRP bars have low modulus of elasticity as well as high tensile and low shear strength [5]. It they do not exhibit any yielding before failure and they behave almost linearly up to tensile rupture. From above, deflections and cracking in FRP RC beams are larger than these found in traditional RC members. The design of FRP RCB is often governed by the serviceability limit states [6,7].

Past papers (studies) showed that cracking, deflection and ultimate load behavior of GFRP reinforced concrete beams can be predicted with the same degree of accuracy as the behavior of regular steel reinforced concrete beams and that a theoretical correlation is therefore possible [8,12]. Basalt fiber-reinforced polymer (BFRP) bars are the newest type of FRP reinforcement used in structural engineering. The mechanical properties of basalt bars are the same to GFRP [13-15]. For that it can be designed according to ACI 440.1R-06 [5]. Nevertheless, BFRP reinforcement is a relatively new material, so behavior of BFRP RC elements should still be thoroughly examined.

Basalt bars has many advantages over steel, galvanized steel and epoxy-coated steel rebar. Basalt bars is less than about 25% the weight of steel rebar, greater than twice the tensile strength of steel, is electrically non-conductive, non-magnetic, insulates against thermal transfer, and of the same thermal coefficient expansion as concrete. The reinforcement ratio has a significant influence on the behavior of flexural strength for BFRP RCB. There is good accuracy between the experimental study and the results obtained from FRP RC flexural members using other metallic reinforcement [16,17,18].

The percentage of service load to the limit loads for beams using BFRP reinforcement are corresponds well with the values which obtained from RC element with other kind of FRP reinforcement [6,19,20]. The main aim of this study was to evaluate the ultimate load, ductility of the beam, max. deflection, the ultimate compration concrete stress, and ultimate tensile force in bars when replacement the traditionally steel reinforced bars by BFRP bars for simply supported RC beams by using (FEM) ANSYS 12.0.

II. Finite Element Model

The analysis of reinforced simple concrete beam strengthened with BFRP bars were modeled using ANSYS 12.0 [21] nonlinear finite element software. ANSYS 12.0. Model components received throughout the

current study, corresponding FE representation and corresponding elements designation in ANSYS are showed as follows:
The nonlinear constitutive law of each material was also implemented in the model.

2-1- Element Type Selection

The three-dimensional hexahedra element SOLID 65 element type with eight corner nodes having three translation degrees of freedom at each node from ANSYS element library is adopted to discretize the concrete beam, which is able to simulate cracking behavior of the concrete under tension (in three orthogonal directions), crushing in compression and evaluate the material non-linearity. The longitudinal, transverse steel and BFRP bars are modeled using LINK 8 element type available in the ANSYS 12.0 element library, which facilitates non-linearity of the material and shows linear deformation in the plane in which it is present.

2.2. Material Modeling

In this study, the components of the concrete beams strengthened with BFRP bars are modeled with germane ANSYS 12.0 elements as follows:

2-2-1- Modeling of Concrete

The concrete was considered as concrete damage plasticity (CDP) material [22], which is based on the brittle-plastic deterioration model [23].
Concrete properties is modeled for SOLID65 element type and it is defined in three stages in ANSYS 12.0 [24] according to the following:

a) Liner elastic isotropic:

- Modulus of elasticity $Ec = 4400\sqrt{f_{cu}}$ (1)
- Poisson's ratio PRXY= 0.20:0.25 for concrete

b) Nonlinear inelastic non-metal plasticity of concrete:

- Open shear transfer coefficient = 0.20 : 0.40
- Closed shear transfer coefficient = 0.80 : 1.00
- Uniaxial cracking stress $f_{ctr} = 0.60\sqrt{f_{cu}}$ (2)
- Uniaxial crushing stress $f_c^{'} = 0.80\, f_{cu}$ (3)
- Biaxial crushing stress = 0.00
- Hydrostatic pressure = 0.00
- Hydrostatic biaxial crush stress = 0.00
- Hydrostatic uniaxial crush stress = 0.00
- Tensile crack factor = 0.00

c) Nonlinear elastic multilinear elastic : for define multilinear isotropic stress-strain curve according to the following formula

For linear curve:

- Point 1(0,0)
- Point 2 $f = \varepsilon.E_c\,;\ \varepsilon = \dfrac{f}{E_c}$ (4)

where ;

$f = 0.30\ f'_c$ (5)

$f'_c = 0.80\ f_{cu}$ (6)

- For rest of curve : from point 3:11

$$f = \frac{E_c.\varepsilon}{1+2\left(\dfrac{\varepsilon}{\varepsilon_0}\right)} \quad (7)$$

where ;

$$\varepsilon_0 = \frac{2 f_c^{'}}{E_c} \qquad (8)$$

The illustrated stress-strain curve for concrete with f_{cu}= 30 N/mm^2 is used for this paper according to strains were assumed and stress was calculated as shown in table 1 according to the previous formula for each strain but, Noted that the last point defined at f'$_c$ & ε=0.0030 indicating that traditional crushing strain.

Table (1) points of stress and strains for stress strain curve to concrete
(F_{cu}=30 N/mm^2, E_c=240998 N/mm^2,F_c'=24 N/mm^2, and ϵ_o=0.003)

Point	ϵ	σ
1	0	0
2	0.0002988	7.200
3	0.0006000	13.257
4	0.0007000	15.015
5	0.0008500	17.329
6	0.0010000	19.248
7	0.0012500	21.612
8	0.0015000	23.067
9	0.0017000	23.702
10	0.0019917	24.000
11	0.0030000	24.000

For concrete under uniaxial compression, the stress-strain curve shown in Fig. 1 was adopted.

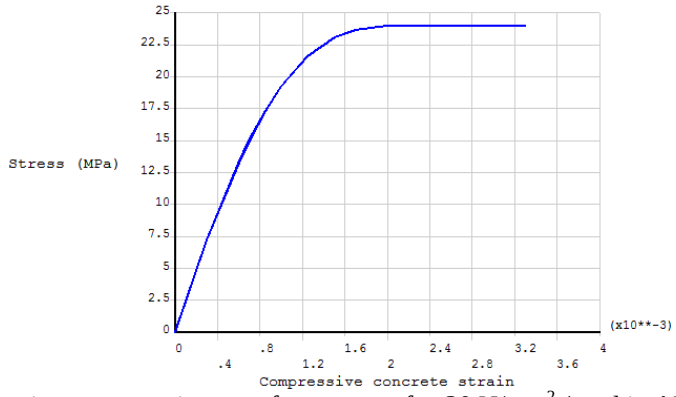

Fig. 1 Compressive stress-strain curve for concrete f_{cu}=30 N/mm^2 (used in ANSYS model)

2-2-2- Modeling of Steel Reinforcement Bars

The bilinear elastic-plastic material stress-strain relationship for steel reinforcement indicated in Fig. 2 is used in this study [25].

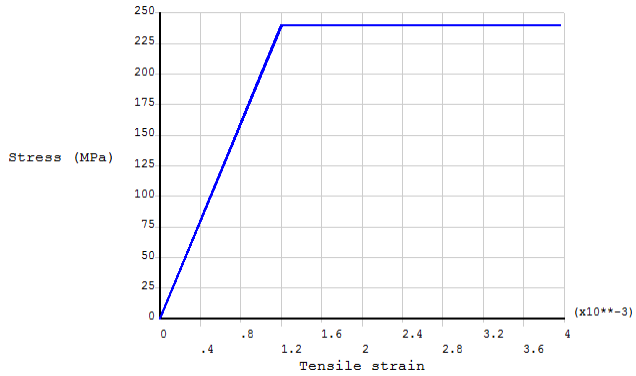

Fig. 2-a Stress-strain curve for steel (grade B240SP)
Stirrups in beam (used in ANSYS model)

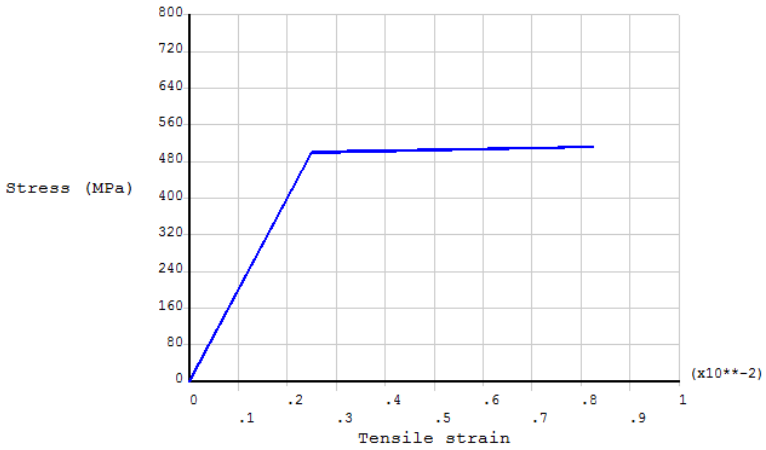

Fig. 2-b Stress-strain curve for steel (grade B500SP)
Top and Bottom Reinforcement in Beam (Used In ANSYS Model)

2-2-3- Modeling Of BFRP Bars

The stress-strain curve for BFRP bars for diameters 7 mm, and 9 mm was assumed as a linear elastic-plastic material with isotropic hardening Fig. 3(a-b) [25].

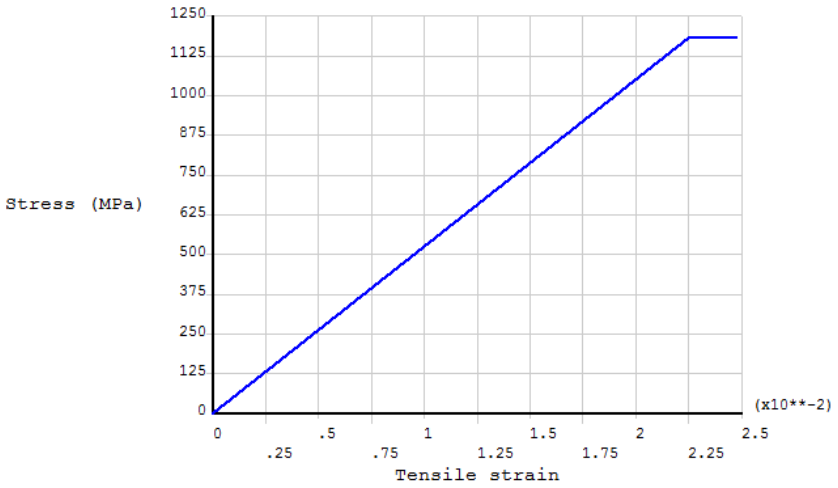

Fig. 3-a Stress-strain curve for bar 7 mm diameter BFRP
(used in ANSYS model)

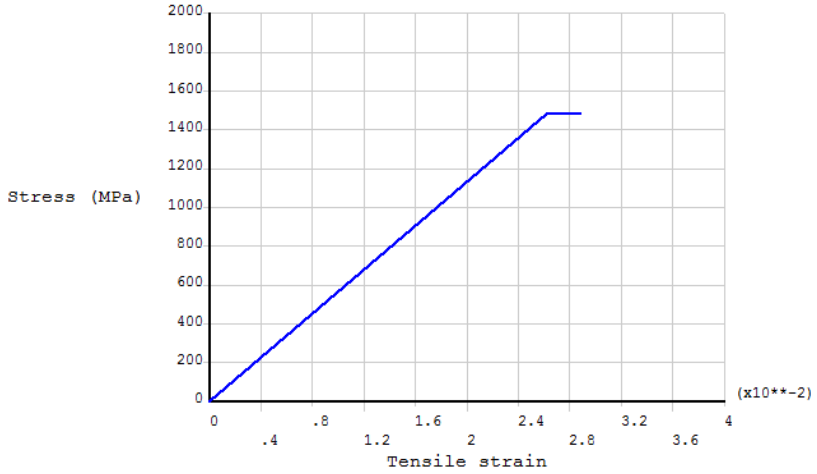

Fig. 3-b Stress-strain curve for bar 9 mm diameter BFRP
(used in ANSYS model)

2-3- Geometrical Modeling and Finite Element Meshing

The numerically modeled for reinforced concrete beams strengthened with BFRP bars are typically simple concrete beams strengthened with BFRP bars as previously discussed. The model is defined by two types of elements that form the concrete beam, reinforcement's bars (steel and basalt). The finite element mesh developed followed the same methodology and degree of refinement presented in Fig. 4(a-c).

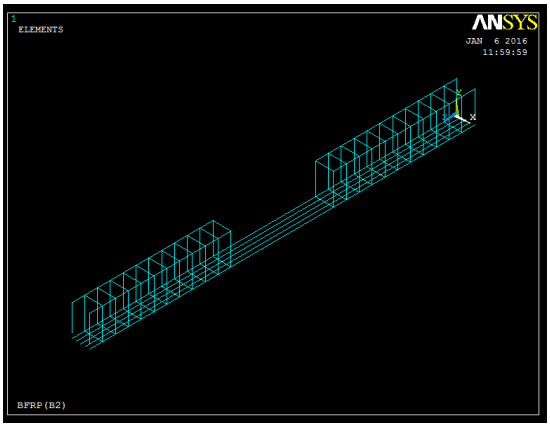

a) Reinf. by Basalt bars, stirrup hanger, and Stirrups for simple beam

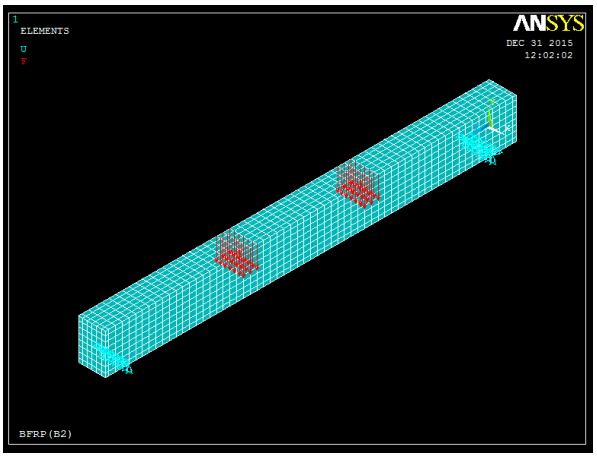

b) Element model and loads

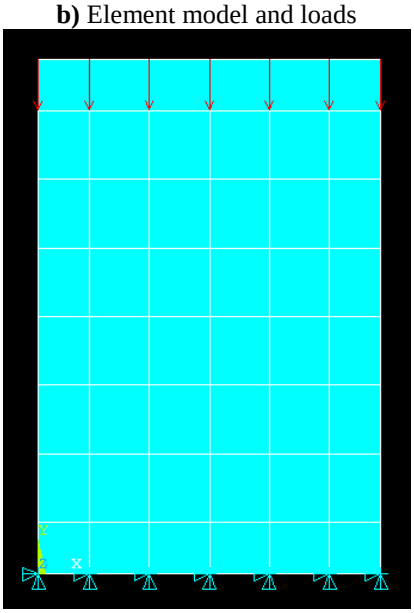

c) Concrete cross section

Fig. (4 a-c) Finite element model for beam (ANSYS)

III. The Validation of the Model

The validation of the model was examined by comparison with experimental results of three simply supported RC beams strengthened with Basalt fiber-reinforced polymer (BFRP) bars carried out by Pawlwsi, and Szumigala [25] with the model. The beams were designed to fail by concrete crushing. Three different amounts of BFRP reinforcement were used for two diameter 7 mm and 9 mm. The designation of the beams designed by ACI 440.IR-06 [5]. The geometry, reinforcement of test beams, parameters and material properties of the concrete beams are shown in, Fig.5 and Table 2 to 4.

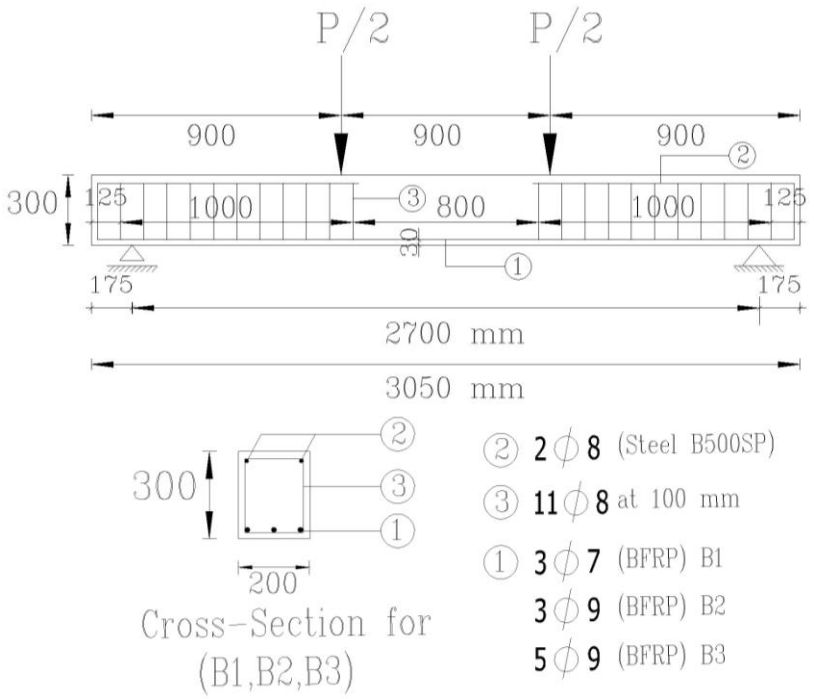

Fig. 5 Concrete beams strengthened with (BFRP) bars

Table (2) Material properties for concrete beams, and steel reinforcement

Concrete Beams			**Steel Reinforcement**		
E_c (GPa)	**f_{cu} (MPa)**	**F_t (MPa)**	**E_s (GPa)**	**f_y** (Stirrups) **(MPa)**	**f_y** (top and bottom) **(MPa)**
24.10	**30.00**	**3.30**	**200.00**	**240.00**	**500.00**

According to PN-EN 1992-1-1 [26], EN-206:2001 [27]

Table (3) Material properties for BFRP ribbed bars [28]

Diameter (mm)	**Nominal diameter (mm)**	**Modulus of elasticity E_B (GPa)**	**Tensile strength F_B (MPa)**	**Ultimate Strain ε_B (%)**
6.74	**7**	**52.8**	**1185**	**22.5**
8.65	**9**	**56.3**	**1485**	**26.2**

Table (4) BFRP Beams Details (B1 to B3)

Beam	**Nominal diameter For (** BFRP **(mm)**	**Reinforcement ratio, ρ(%)**
B1	**3 Ø 7**	**0.19**
B2	**3 Ø 9**	**0.32**
B3	**5 Ø 9**	**0.54**

Figures 6-11 show the shape of mid-span deflection, concrete stress intensity distribution, and ultimate compressive strength of concrete along the beams (B1, B2, and B3) respectively by ANSYS. Figures 12-13 indicate the experimental and analytical results of Mid-span deflection distribution along the beams (B1, and B3). As can be observed in table 5, the ultimate load, and max. deflection for three beams. The failure modes for beams shown in table 6, for beam one is duo to Reinforcement Rupture, for beam two duo to Reinforcement Rupture in Stirrups and Concrete Crushing, and for beam three duo to Reinforcement Rupture in Stirrups.

It is shown from these figures and table that the results obtained by finite element model using ANSYS 12.0 have a good agreement with experimental results.

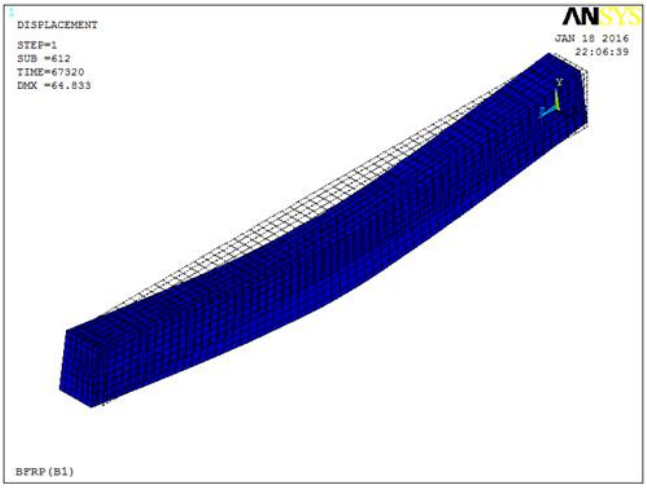

Fig. 6 Shape of Deflection Distribution along beam (B1)

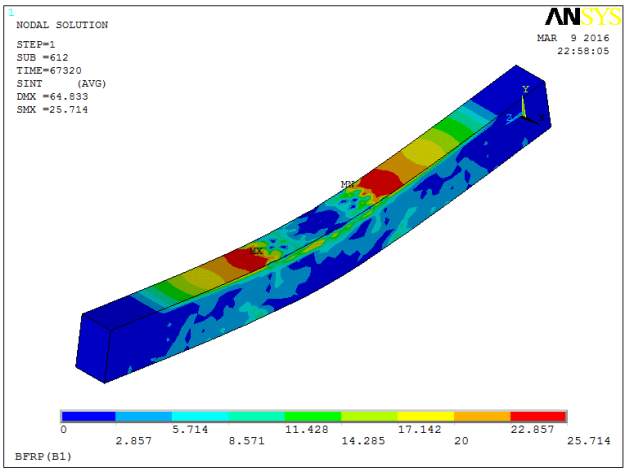

Fig. 7-a Shape of Concrete Stress Intensity Distribution along (B1)

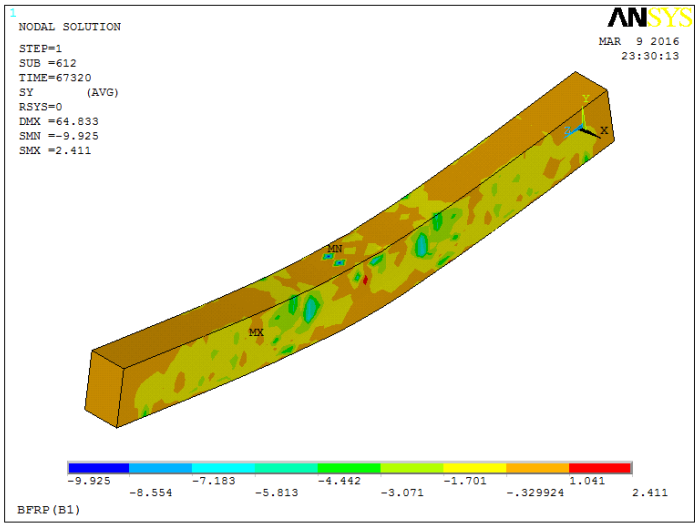

Fig. 7-B Shape of Ultimate Compressive Strength of Concrete for (B1)

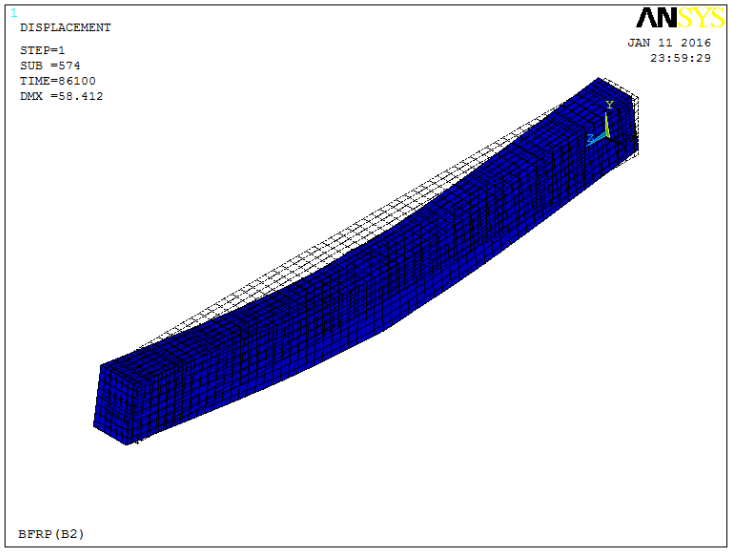

Fig. 8 Shape of Deflection Distribution along Beam (B2)

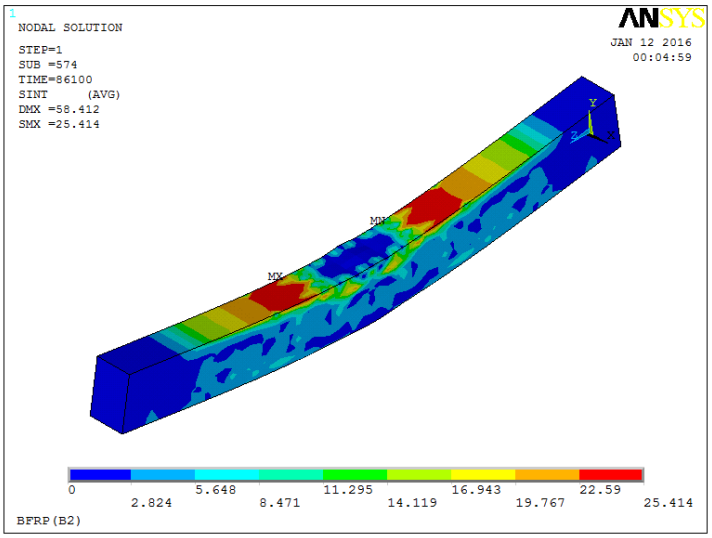

Fig. 9-a Shape of Concrete Stress Intensity Distribution along (B2)

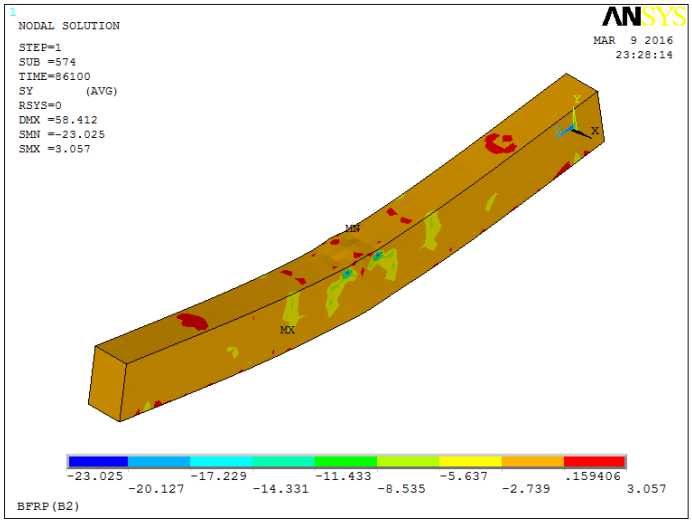

Fig. 9-B Shape of Ultimate Compressive Strength of Concrete for (B2)

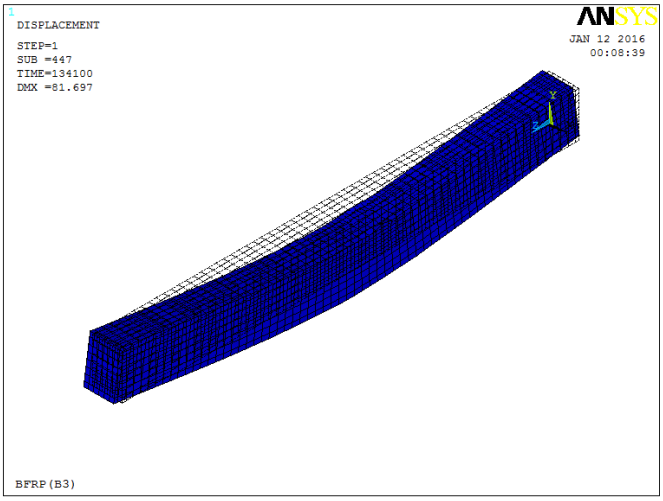

Fig. 10 Shape of Deflection Distribution along beam (B3)

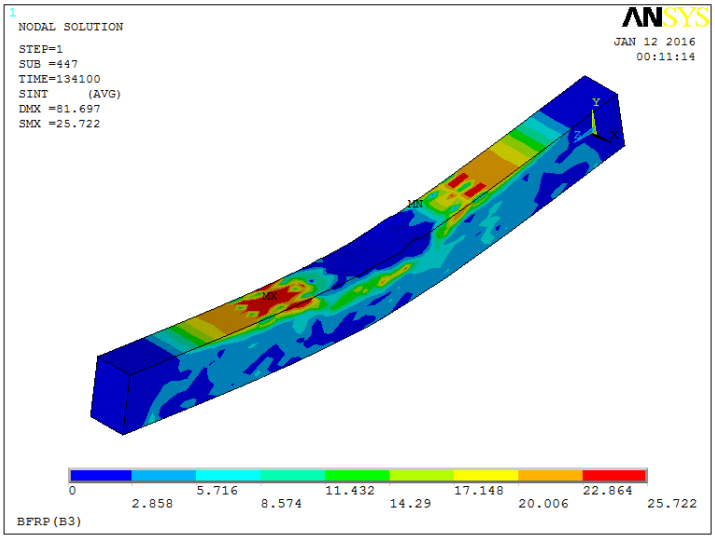

Fig. 11-a Shape of Concrete Stress Intensity Distribution along (B3)

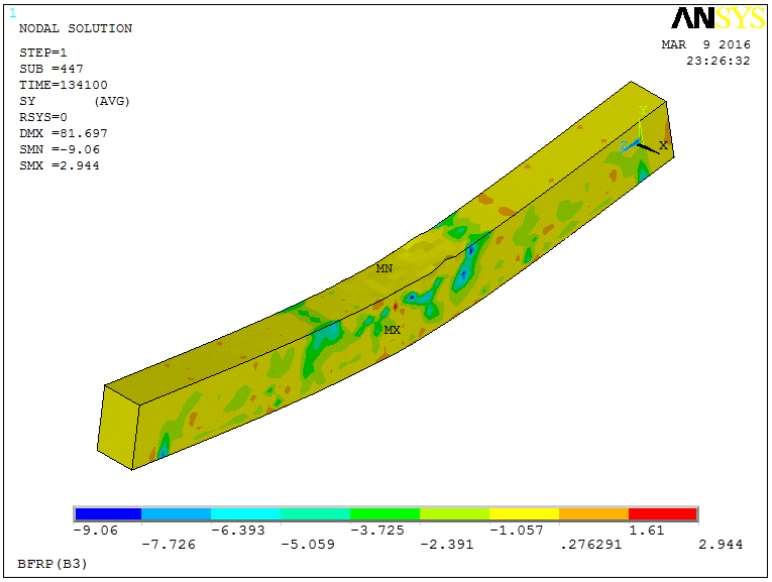

Fig. 11-B Shape of Ultimate Compressive Strength of Concrete for (B3)

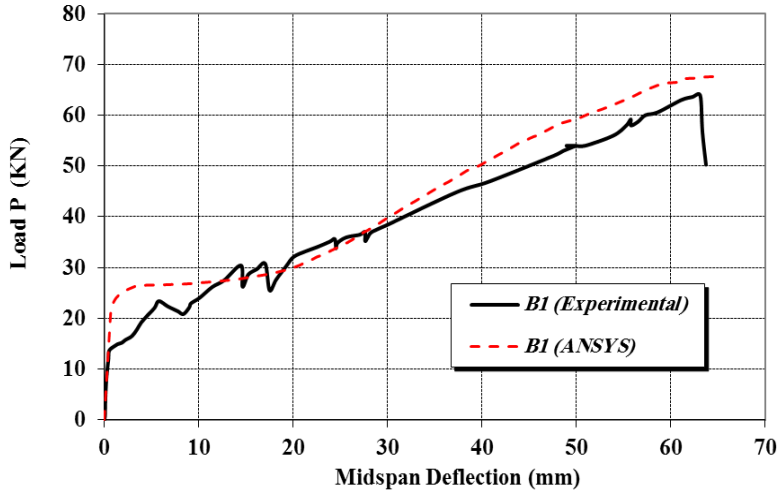

Fig. 12 Load versus Mid-span Deflection distribution for (B1)

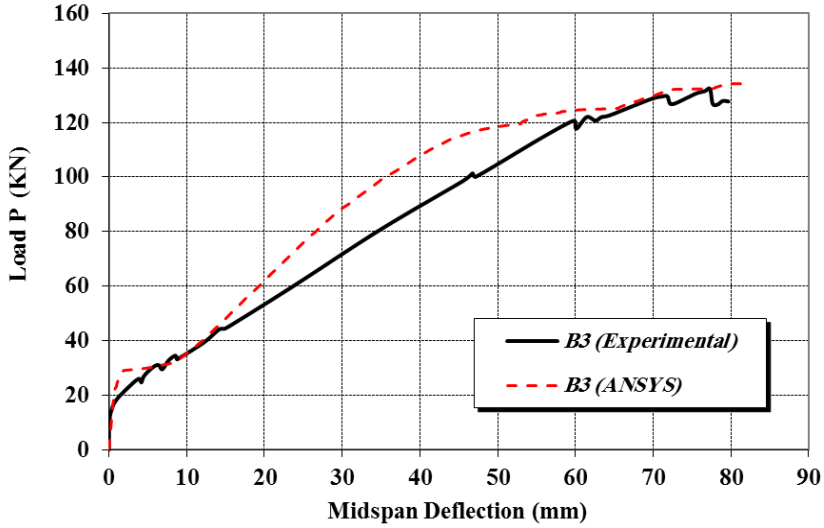

Fig. 13 Load versus Mid-Span Deflection Distribution for (B3)

Table (5) Comparison between Experimental and FEA (ANSYS) for beams B1, B2, and B3

Beam	Ultimate Load Pu (KN)		Max. Def. Δ (mm)	
	Experimental	ANSYS	Experimental	ANSYS
B1	63.9	67.3	63	64.8
B2	85.9	86.2	›58	58.4
B3	132.3	134.1	78	81.6

Table (6) Failure mode between Experimental and FEA (ANSYS) for beams B1, B2, and B3

Beam	Failure mode	
	Experimental	ANSYS
B1	RR	RR
B2	RR&CC	RR,CC
B3	CC	RR

RR= Reinforcement Rupture & CC= Concrete Crushing

IV. Parametric Study

As illustrated in previously, Finite element models performed with numerical analysis using ANSYS 12.0 predict truly the analysis and discussion of reinforced concrete beams strengthened with BFRP. Thus, it is possible to perform a parametric study with numerical finite element model followed by indications as illustrated previously. Data, detailed information, and factors affecting on the behavior of reinforced concrete beams strengthened with BFRP were provided with parametric study, thus important conclusions can be

summarized and obtained clearly. The characteristics of the specimens analyzed in the parametric study are illustrated as follow:

Group one for ten control reinforced concrete beams (with traditional reinforcement bars). The first five beams from **B_1S4**, to **B_1S8** are loaded by one point load in its mid-span. The second five beams from **B_2S9**, to **B_2S13** are loaded by two point loads in its third-span.

Group two as the group one but from **B_1B14** to **B_2B23** but replacement the traditional reinforcement bars by BFRP bars.

Materials used; concrete, steel bars and BFRP bars are of the same properties as those used in verification (the stress strain curve for BFRP **Ø 13** as the BFRP **Ø 9).** The Reinforcement ratio shown in table 7, and the details of beams are shown in table 8.

Table (7) Reinforcement ratio **(ρ)** for Beams

Nominal diameter For bars (mm)	Reinforcement ratio ρ(%)
3 Ø 7	**0.19**
3 Ø 9	**0.32**
5 Ø 9	**0.54**
3 Ø 13+2 Ø 9	**0.88**
5 Ø 13	**1.11**

Table 8 Specimens Analyzed in Parametric Study for Beams

Beam	Reinf. type	No. of Lower Reinf.	Loading type
B_1S4	Steel Bars	3Ø7	Series (1) one point loads
B_1S5		3Ø9	
B_1S6		5Ø9	
B_1S7		3Ø13+2Ø9	
B_1S8		5Ø13	
B_2S9	Steel Bars	3Ø7	Series (2) two points loads
B_2S10		3Ø9	
B_2S11		5Ø9	
B_2S12		3Ø13+2Ø9	
B_2S13		5Ø13	
B_1B14	BFRP	3Ø7	Series (3) one point loads
B_1B15		3Ø9	
B_1B16		5Ø9	
B_1B17		3Ø13+2Ø9	
B_1B18		5Ø13	
B_2B19	BFRP	3Ø7	Series (4) two points loads
B_2B20		3Ø9	
B_2B21		5Ø9	
B_2B22		3Ø13+2Ø9	
B_2B23		5Ø13	

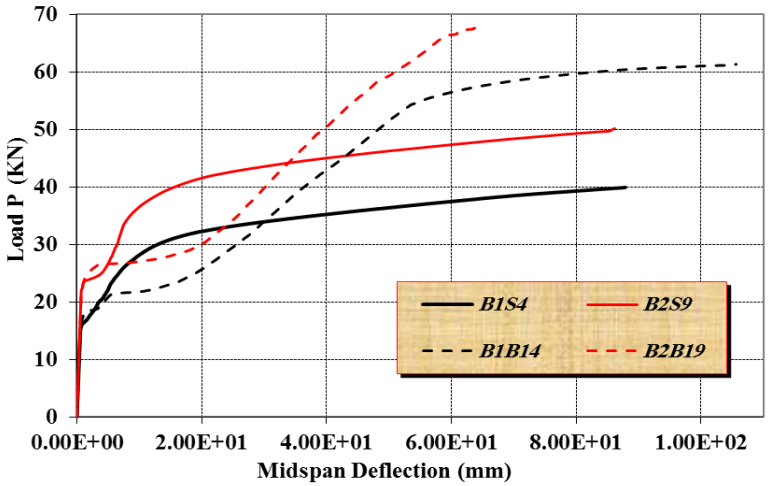

Fig. 14 Load versus mid-span deflection for beams (ρ=0.19)
$BS_1$4, $BS_2$9, $BB_1$14, and $BB_2$19

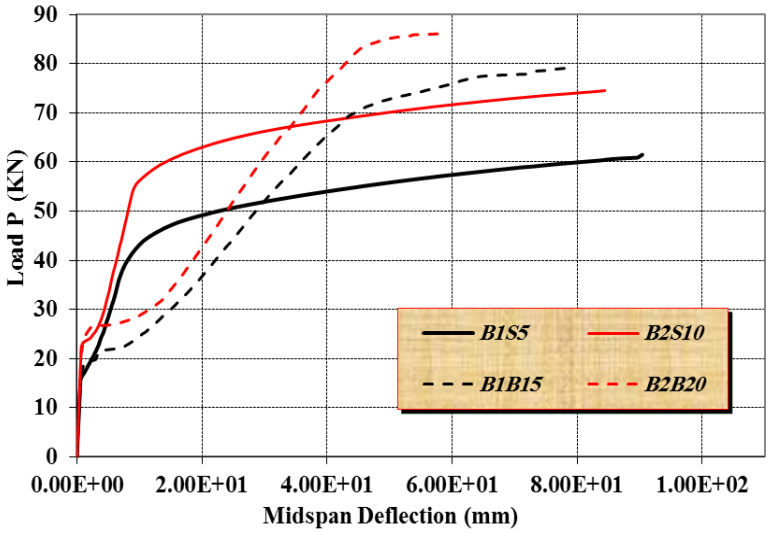

Fig. 15 Load versus mid-span deflection for beams (ρ=0.32) $BS_1$5, $BS_2$10, $BB_1$15, and $BB_2$20

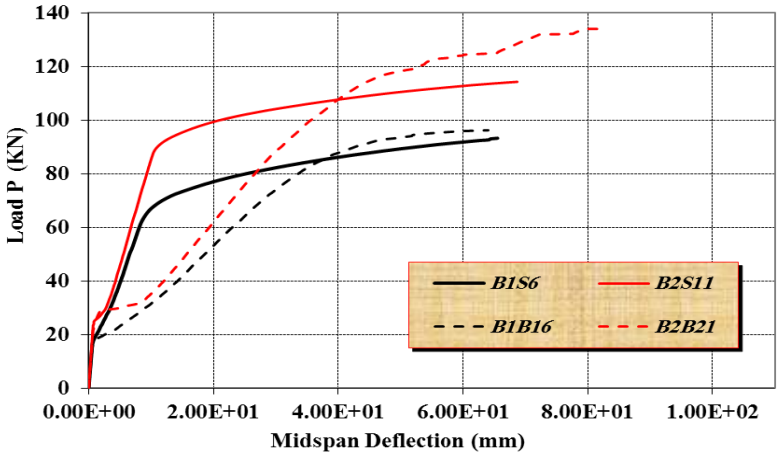

Fig. 16 Load versus mid-span deflection for beams (ρ=0.54) $BS_1$6, $BS_2$11, $BB_1$16, and $BB_2$21

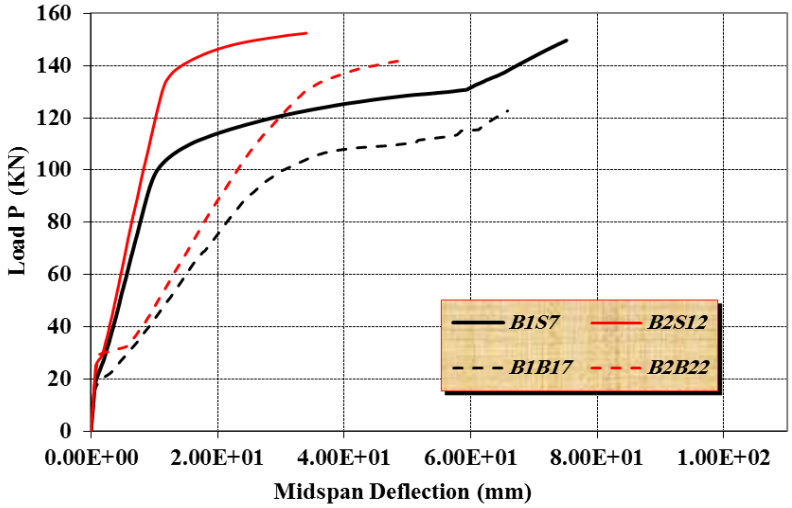

Fig. 17 Load versus mid-span deflection for beams (ρ=0.88) $BS_1$7, $BS_2$12, $BB_1$17, and $BB_2$22

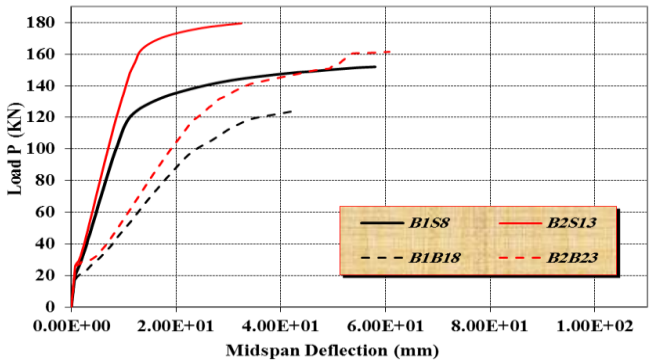

Fig. 18 Load versus mid-span deflection for beams (ρ=1.11)
$BS_1$8, $BS_2$13, $BB_1$18, and $BB_2$23

4-1- Failure Mode and Ultimate Load of the Beams

Table 9 shown the ultimate load, max. Def., ultimate tensile force bars, ultimate compration concrete stress, and failure mode for beams **(B_1S4 to B_2B23)**

Table 9 Deflection and Service Loads for Beams ($BS_1$4 to $BB_2$23)

Beam	Ultimate load P_u (KN)	Max. Def. Δ (mm)	Ultimate tensile force bars (KN)	Ultimate Compration Concrete stress (N/mm^2)	Failure mode
B_1S4	40.04	90.60	25.41	5.98	**RRb**
B_1S5	61.65	92.80	40.89	8.35	**RR**b
B_1S6	93.60	67.16	37.98	13.35	**RRb**
B_1S7	150.00	76.30	72.76&36.50	10.15	**RRb**
B_1S8	152.50	59.73	70.51	22.83	**RR**b
B_2S9	50.27	88.71	23.66	4.15	**RRb**
B_2S10	74.70	86.60	37.46	6.25	**RR**b
B_2S11	114.60	71.01	35.11	7.62	**RRb**
B_2S12	152.80	35.98	66.45&33.22	10.31	**RRb**
B_2S13	180.00	34.28	65.77	20.77	**RRb**
B_1B14	61.38	109.24	45.59	10.31	**RRb**
B_1B15	78.90	77.51	75.13	12.06	**RR**s
B_1B16	96.60	65.54	57.08	42.56	**CC**
B_1B17	123.20	66.95	103.54&53.21	18.67	**RR**b
B_1B18	124.50	43.46	74.45	7.69	**RRs**
B_2B19	67.32	64.83	45.124	7.36	**RRb**
B_2B20	86.20	58.41	59.83	23.03	**RRs&CC**
B_2B21	134.10	81.60	71.71	9.06	**RRs**
B_2B22	142.40	51.10	87.56&43.24	7.93	**RRb**
B_2B23	162.00	64.03	90.14	11.11	**RRs**

RRb= Reinforcement Rupture bars & RRs= Reinforcement Rupture Stirrups & CC= Concrete Crushing

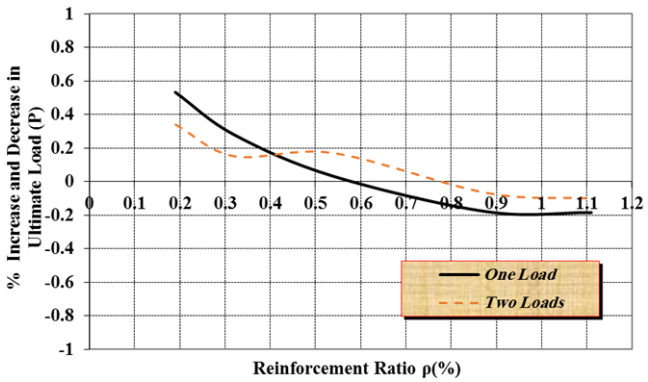

Fig. 19 Percentage of Increasing and Decreasing for Load {of BFRP with respect to traditional steel} to Reinforcement Ratio in beams

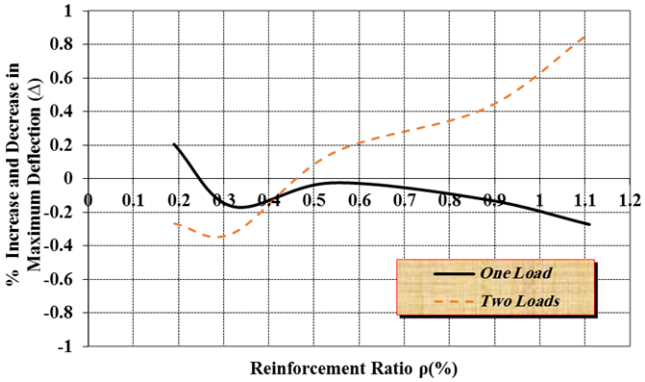

Fig. 20 Percentage of Increasing and Decreasing for deflection {of BFRP with respect to traditional steel} to Reinforcement Ratio in beams

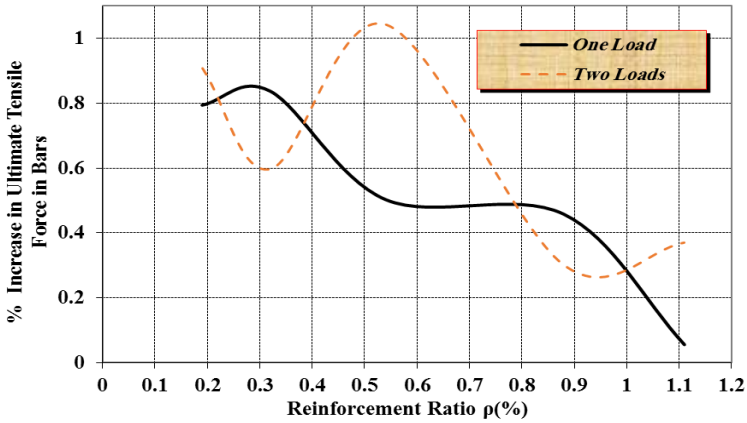

Fig. 21 Percentage of Increasing and Decreasing for Ultimate tensile Force Bars {of BFRP with respect to traditional steel} to Reinforcement Ratio in beams

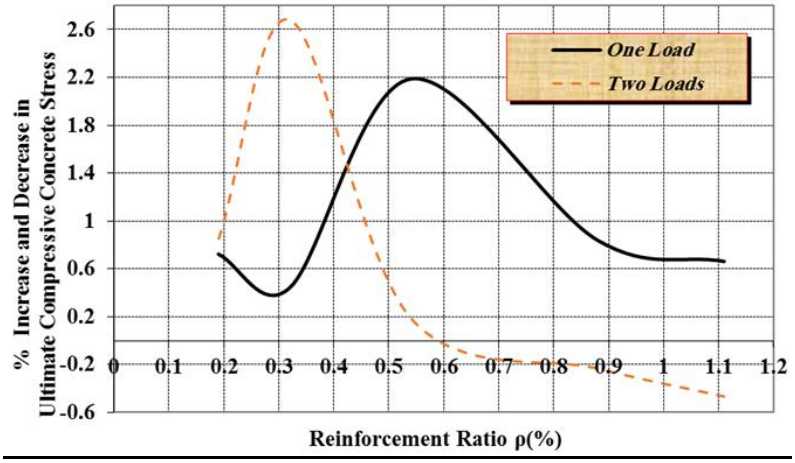

Fig. 22 Percentage of Increasing and Decreasing for Ultimate Compressive Concrete Stress {of BFRP with respect to traditional steel} to Reinforcement Ratio in beams

4-2- Ultimate Load

Figures 14 to 18 shows the load versus mid-span defection for the case of one and two concentrated loads for beams using steel bars, and BFRP bars. And Fig. 20 show the percentage of increasing and decreasing ultimate load to reinforcement ratio. Figure 19 show that, the replacement of steel reinforcement with BFRP bars increase the ultimate load 53% in case of one concentrated load, and to 34% in case of two concentrated load in the case minimum reinforcement ration 0.19%. This increasing percentage decrease gradually to reach zero at reinforcement ratio 0.58% in case of one load and 0.78% in case of two concentrated load. After that decrease the ultimate load.

For that the BFRP is effective than the traditional steel bars at reinforcement ratio less equal 0.58% in case of one load and 0.78% in case of two concentrated load.

4-3- Deflection

Figure 20 show that, the replacement of steel reinforcement with BFRP bars decrease the max. deflection 30 % in case of one concentrated load, But increase about 81% in case of two concentrated load, because the ultimate load in case of two concentrated loads is higher and all that in case of higher reinforcement ratio 1.1%.

4-4- Ultimate Tensile Force in Bars

Figure 21 show that, the replacement of steel reinforcement with BFRP bars increase the ultimate tensile force basalt bars 82% at reinforcement ration 0.3% and 104% at reinforcement ration 0.52% in cases of one and two concentrated load respectively. The increasing percentage in one and two case of loading equals at reinforcement ration at 0.22%, 0.39%, 0.78%, and 1%, and in case of one concentrated load this percentage below after reinforcement ration 1%.

4-5- Ultimate Compressive Concrete Stress

Figure 22 show that, the replacement of steel reinforcement with BFRP bars increase the ultimate compration concrete stress 220% at reinforcement ration 0.55% and 262% at reinforcement ration 0.32% in cases of one and two concentrated load respectively. The increasing percentage in one and two case of loading equals at reinforcement ration at 0.19%, 0.42%, 0.78%, and 1%. This percentage lese at grater reinforcement ration, and its decreasing (opposite) after reinforcement ration 0.6% in case of two concentrated load only.

4-6- Failure Modes

All most failure modes are in reinforcement bars (bottom steel or BFRP or steel stirrups). Since the main study in this paper is to show the effect of BFRP in RCB.

At reinforcement ration 0.4% the increasing percentage in ultimate load, decreasing percentage max. deflection, increasing percentage ultimate tensile force bars, and increasing percentage ultimate compration concrete stress are equal for RCB with steel bars, or BFRP, or in case of loaded the simple beam by one or two concentrated loads.

V. Conclusion

In the research work, a finite element approach for the nonlinear analysis of beams with BFRP bars has been presented. The following remarks were concluded.

1. Three failure modes were illustrated during test of specimens Reinforcement Rupture bars, Reinforcement Rupture Stirrups, and Concrete Crushing.
2. The Rein. Ratio has a significant effect on the stiffness of the BFRP RC beams (flexural behaviour). Since increase the ultimate load about 258 % in case of one concentrated load to 281 % in case of two concentrated load for steel bars and about 103% to 141% in case of BFRP.
3. The replacement of steel reinforcement with BFRP bars increase the ultimate load, from about 53 % to 34 % in cases one and two concentrated loads respectively.
4. The increasing percentage in ultimate load decreasing by increasing reinforcement ration.
5. The replacement of steel reinforcement with BFRP decrease the max. deflection, from about 30 % to 81 % in cases one and two concentrated loads respectively.
6. The behaviour of RC beams strength with BFRP bars is linearly until failure.
7. Design of the BFRP beams is governed by the serviceability limit states.
8. It can be seen that for BFRP bras beams, significant increase in load capacity is achieved by using two loads rather than one load. This can be predicted as using two loads result in less moment and so less deformation compared to that developed by using one load.

References

[1]. Sarja A. Intergrated life cycle design f structures. New York: Spon Press, 2002.
[2]. PCA. Types and Causes of concrete deterioration. IS536, Portland Cement Association, 2002.
[3]. Fib Bulletin 40/2007. FRP Reinforcement in RC structures, technical report. International Federation for Structural Concrete (fib). September 2007, p. 3-30.
[4]. Fib Bulletin 40/2007. FRP Reinforcement in building construction. Przeglad Budowlany 2014;3: p. 47-50 (in Polish).
[5]. ACI Guide for the design and construction of structural concrete reinforced with FRP bars. ACI 440.1R-06, American Concrete Institute, 2006.
[6]. Barris C, Torres L, Tauron A, Baena M, Catalan A. An experimental study of the flexural behaviour g GFRP RC beams and comparison with prediction models. Composites Structures 2009; 91: p. 286-295.

[7]. Nanni A. North American design guidelines for concrete reinforcement and strengthening using FRP: principals, applications and unresolved issues. Construction and Building Materials 2003; 17(6-7): p. 439-446.
[8]. Wang, X., Wang, W.W., Dai, J.G. and Zhao, F. (2012), FE Analysis of GFRP-Concrete Composite Bridge Decks Using a Mixed Element Approach, Proceedings of the Fourth Asia-Pacific Young Researchers & Graduates Symposium: The Future of Structural Engineering- Research, Practice and Education, 5-6 December, Hong Kong, China, p.169-174.
[9]. Sun, X.Y., Dai, J.G., Wang, H.L. and Xu, C. (2012), Static and Fatigue Behavior of CFRP-strengthened RC Beams Subjected to Overloading, Proceeding of the First International Conference on Performance-based and Life-cycle Structural Engineering (PLSE2012), 5-7 December, 2012, Hong Kong, CD-ROM, p.725-733.
[10]. Wang, G. L., Dai, J. G. and Teng, J. G. (2012), Shear Strength Model for RC Beam-Column Joints under Seismic Loading, Engineering Structures, 40, 350-360. (SciVerse Top 25 Hottest Articles Engineering Structures, April to June 2012).
[11]. Dai, J. G., Ueda, T., Sato, Y. and Nagai, K. (2012), Modeling of Tension Stiffening Behavior in FRP-Strengthened RC Members Based on Rigid Body Spring Networks, Computer-Aided Civil and Infrastructure Engineering, 27(6), p. 406-418.
[12]. Wang, W.W., Dai, J. G., Harries, Kent, A. and Bao, Q.H.(2012), Prestress Losses and Flexural Behavior of Reinforced Concrete Beams Strengthened with Post-tensioned CFRP Sheets, Journal of Composites for Construction, ASCE, 16(2), p. 207-216.
[13]. Schock Bauteile GmbH. Gerrmany. March 2015. http://www.schoeck-combar.com/
[14]. Polprek Sp. Zo.o. Poland. March 2015. http://www.polprek.pl/start
[15]. Garbacz A, Lapko A, Urbanski M. Investigation on concrete beams reinforced with basalt rebars as an effective alternative of conventional R/C structures. Proceedingos f the 11th International Conference on Modern Building Materials, Structures and Techniques. Procedia Engineering 2013;57: p.1183-1191.
[16]. Barris C, Torres L, Comas J, Mias C. Cracking and deformation in GFRP RC beams: an experimental study. Composites: part B 2013; 55: p. 580-590.
[17]. Shour A F. Flexural and shear capacities of concrete beams reinforced with GFRP bars. Construction and Building Materials 2006; 20: p. 1005-1015.
[18]. Adam M, Said M, Mahmoud A, shanour A. Analytical and experimental flexural behavior of concrete beams reinforced with glass fiber reinforced polymers bars. Construction and Building materials 2015; 84:p. 354-366.
[19]. Barris C, Torres L, Mias C, Vilanova I. Design of FRP reinforced concrete beams for serviceability requirements. Journal of Civil Engineering and Management 2012; 18(6): p. 843-857.
[20]. Alsayed SH, Al-Salloum Y, Almusallam TH. Performance of glass fiber reinforced plastic bars as a reinfoecing material for concrete structures. Composites: Part B 2012; 31: p. 555-567
[21]. ANSYS 12.0 User Manual Revision , ANSYS Inc., Canonburg, Pennsylvania, USA, 2009.
[22]. Lubliner J, Oliver J, Oller S, Onate E. A plastic-damage model for concrete. International Journal of Solids Mechanics 1989; 25: p. 299-326.
[23]. Lee J, Fenves GL. Plastic-damage model for cyclic loading of concrete structures. Journal of Engendering Mechanics 1998; 124: p. 892-900.
[24]. Wang T, Hus TTC. Nonlinear finite element analysis of concrete structures using new constitutive model. Computer and structures 2001: 79: p. 2781-2791.
[25]. Pawlowski, D, Szumigala M. Flexural behavior of full-scale basalt FRP RC beams-experimental and numerical studies. Procedia Engineering 2015: 108: p. 518-525.
[26]. CEN. Design of concrete structures. Part 1-1. General rules and rules for building. EN 1992-1-1:2004. Comite Europeen de Normalisation Brussels, 2004.
[27]. CEN Concrete –Prat 1 Specification, performance, production and conformity. EN-206-1. Comite Europeen de Normalisation Brussels, 2000.
[28]. Kaminska M. The results of tests of composite bars made of BFRP and GFRP. Lodz University of Technology, 2012 (in polish).